Effect of Geometrical Parameters of Aluminum-to-Steel Bolted Connections

Thérèse A. D. Tajeuna[1*], Frédéric Légeron[2], Pierre Labossière[3], Marc Demers[4] and Sébastien Langlois[5]

[1] Ph.D Student
Department of Civil Engineering
University of Sherbrooke, Sherbrooke, Quebec, Canada, J1K 2R1
E-mail: **Therese.Tajeuna@USherbrooke.ca**

[2] Professor
Department of Civil Engineering
University of Sherbrooke, Sherbrooke, Quebec, Canada J1K 2R1
E-mail: **Frederic.Legeron@USherbrooke.ca**

[3] Professor
Department of Civil Engineering
University of Sherbrooke, Sherbrooke, Quebec, Canada J1K 2R1
E-mail: **Pierre.Labossiere@USherbrooke.ca**

[4] Research Engineer
Department of Civil Engineering
University of Sherbrooke, Sherbrooke, Quebec, Canada J1K 2R1
E-mail: **Marc.Demers@USherbrooke.ca**

[5] Assistant Professor
Department of Civil Engineering
University of Sherbrooke, Sherbrooke, Quebec, Canada J1K 2R1
E-mail: **Sebastien.Langlois@USherbrooke.ca**

[*]Author to whom all correspondence should be addressed

Paper to be submitted to Engineering Structures (Elsevier)

ABSTRACT

Through experimental and numerical studies, this research work aims to provide directions on the optimal geometric configuration for single-lap and double-lap bolted connection between aluminum alloy 6061-T6 and steel. From experimental test results, the effects of different geometric parameters on the joint strength were discussed. These parameters include the end-distance, the side-distance, the pitch-distance, the plate thickness and the joint eccentricity. Then, the experimental results were compared to predicted results using design references and geometric recommendations proposed by design references were critically examined. The experimental study was complemented by finite element (FE) analysis to extend the study to a larger range of parameters. In addition to the analysis of the geometric parameters listed above, the effects of the gage-distance on the joint strength were studied in the FE analysis. The experimental and finite element results show that a careful selection of geometric parameters can result in the high improvement of the connection strength and failure mode. Limiting the side-distance to the minimum recommended value was found to limit the strength of a connection with two bolts in a column to that of the one-bolt connection. In most cases, bearing was found to govern the strength of the connections. The calculated bearing strengths were found to underestimate significantly the connection strength. Based on these analyses, maximum geometric parameters beyond which there is no further increase of the joint capacity were evaluated and optimum geometric parameters were proposed.

Keywords: Bolted connection, aluminum, geometric parameters, single-lap, double-lap, design prediction, finite element.

1. Introduction

This study was initiated in the context of developing a high strength and low weight portable emergency bridge for railways. The use of aluminum members is a promising option for

secondary elements in such bridges due to their light weight, corrosion resistance, and low maintenance cost. Aluminum alloy 6061 is easily available and used for many applications. It can be employed without painting if exposed to general atmospheric corrosion. However, when aluminum is attached to steel components, painting the steel components and placing an electric isolator in the joint are required to prevent galvanic corrosion. A critical aspect to consider for the efficient use of aluminum for portable structures is the behavior of aluminum-to-steel connections. In particular, designers would need to optimize the geometric configurations of those connections.

1.1. Research objective

The main objective of this research is to provide basic information on the static behavior of aluminum to steel joint in civil engineering applications, compare the experimental results to predicted results using design references, critically examined the geometric recommendations proposed by design reference and to evaluate the maximum geometric parameters beyond which there is no further increase of the joint capacity. This paper is divided into four parts: In the first part, a literature review of aluminum bolted joint is presented. Then, the static test of single-lap and double-lap bolted joints using varying geometric parameters in one and two bolts joints is experimentally studied. Next, calculated joint strengths using equations from three different references, namely Eurocode 9 (EC9) [1], AASHTO LRFD Bridge Design Specifications (AASHTO) [2], and Strength design in aluminum/Commentary on CSA S157-05 (CSA-S157) [3] are compared to experimental results. Finally, finite element analysis validated by experimental results is used to extend the data to a large range of parameters. Based on these different analyses, optimum geometric parameters are proposed for one-bolt and two-bolt connections.

2. Literature review

Among the different joining techniques, bolting appears to be the most practical choice for emergency portable bridges as it can be easily disassembled. However, bolts introduce stress concentration around the bolt-hole where failure can be initiated. When the components are axially loaded, bearing failure, shear tear-out failure, rupture of the net-section, rupture by block shear, yielding of the gross-section and shear failure of the bolt are the six possible modes in which the loaded members can fail. Figure 1 illustrates these six possible failure modes. Equations to calculate the strength for all these failure modes are given in design references. The three design references of interest in this study are: EC9 [1], AASHTO [2] and CSA-S157 [3].

Figure 2(a) presents an example of bolted connections loaded in single-lap and double-lap configurations. In a bolted connection, geometric parameters include: the number of shear planes x, end-distance e, side-distance s, width w, pitch-distance p, gage-distance g, plate thickness t, bolt-hole diameter d_h, bolt diameter d, the number of bolts in the row n, the number of bolts in the column m, and the total number of bolts in the connection N. Design references recommend minimum and maximum values for these parameters for the connection of aluminum sections. Table 1 summarises these values for e, s, p and g. The recommended minimum distances may be governed by the clearance for bolt heads and driving tools, as indicated in CSA-S157 [3] while, the maximum are governed by local plate buckling and plate thickness. As presented in Table 1, these maximum and minimum can differ from one design reference to another.

The main objective of the experimental studies available in the literature is the prediction of the behavior of the aluminum connection for different configurations. Menzemer et *al*. [4] performed an experimental investigation to establish criteria to estimate the block shear limit state of bolted connection elements. Block shear failure was found to occur by a tensile fracture in the gage-distance of the first inner row and a more gradual shear failure along each

bolt column. Based on their experimental results, an approach to incorporate the connection length into the effective shear strength was proposed. In another paper, Menzemer et *al*. [5] investigated the bearing strength of three aluminum alloys (5052-H32, 5454-H34 and 3003-H16). Among the key finding, the average ratio of bearing strength to material tensile strength (σ_b/f_u) was higher in configurations with inner aluminum plate than configurations with aluminum outer plates. The effect of bolt pre-load was more relevant in configurations with inner aluminum plate than in configurations with two outer aluminum plates. However, the clamping effect provided either by the bolt pre-load or by the rigidity of the steel cover severely limited the permanent hole elongation. Bearing performance of aluminum bolted connections was also investigated by Wang et *al*. [6], this time for alloys 6061-T6 and 6063-T5. Bolt-diameter and end-distance were the two parameters studied in the experimental analysis while numerical simulations included also the study of plate thickness. Bearing strength of aluminum was found to be directly proportional to bolt-diameter and sheet thickness. With the increase of end-distance, failure mode was found to change from shear to bearing failure. Bearing strength was linearly proportional to the end-distance up to e=3d. Above this value, bearing strength increasing rate was slower. Based on these results, a simplified relation was proposed to evaluate the impact of the end-distance on bearing strength. The effect of end-distance was also investigated by Kim et *al*. [7] for single-lap aluminum 6061-T6 plates joined with four bolts all arranged in 2 rows and 2 columns. The joint strength was found to increase with the end-distance up to 5d. Above this value, a reduction of the joint strength was observed due to the excessive out-of-plane deformation (*curling*). Compared to experimental results, the block shear strengths calculated using AISI-S100 [8] and ADM [9] design specifications were underestimated while for curled specimens the design specifications tended to overestimate the joint strength due to the reduction of the capacity caused by curling. Following their experimental study, Kim et *al*. [10] also

performed a numerical simulation to estimate the structural behavior such as ultimate strength, fracture and out of plane deformation (*curling*) effect on single-lap aluminum bolted connections. From their parametric study, the necessity to consider this effect in the design of joint strength with long end-distance and side-distance was highlighted. From Tinl et *al*. [11] study, the average bearing ratio (σ_b/f_u) at failure of aluminum alloys 5052-H32 and 6061-T6 was found to be equal to 1.6 for e =1.5d and 1.2 for e =1.25d. Compared to the design provisions given by ADM [9] the experimental strengths were found to be larger than the calculated bearing strength using guaranteed minimum mechanical properties.

In summary, many values for the spacing of bolts in connections between aluminum plates have been recommended and can also be found in standards. However, except for the end-distance, maximum geometrical parameters beyond which there is no further increase of the joint capacity are not clearly identified. For instance, Kim et *al*. [10] study indicates that in a four-bolt connection, there is no gain in capacity beyond 5d. This suggests that there is still a need to further investigate the geometrical configuration of the joints, especially the maximum distances between bolts, or between bolts and plate edges, in order to optimize the strength of the connection.

3. Experimental program

3.1. Overview

The static test of few experimental configurations was performed in order to understand the behavior of aluminum to steel bolted connections and to obtain sufficient data to validate the FE model. For this investigation, connections with one-bolt loaded in single-lap and double-lap configurations and two-bolt in a column loaded in single-lap configurations were tested. Five configurations were tested for one-bolt single-lap joint. For the first three configurations, s and e equal 1.5d with plate thickness (t) equal to 3.175 mm (T3), 6.35 mm (T6) and 9.525 mm (T9). For the fourth configuration, s and e were taken at 1.5d and 2d respectively with

155 t=6.35 mm while for the fifth configuration s and e equal 2.5d and t=6.35 mm. Results were
156 used to investigate the effect of s, e and t on one-bolt connections. Then, the effect of joint
157 eccentricity on one-bolt connections was studied by comparing results from the single-lap to
158 those of double-lap with the same end-distance, side-distance and plate thickness (e=1.5d,
159 s=1.5d, t=6.35 mm). Finally, the effect of s on the two-bolt single-lap joint strength was
160 studied. A configuration with e=3d, s=2.5d and p=3d was compared with another
161 configuration for which e=2.5d, s=3d and p=3d both having t=6.35 mm. Specimens were
162 named with respect to their respective geometric parameters. For example, S15E15T9 stands
163 for single-lap one-bolt joint with s=1.5d, e=1.5d and 9.525 mm thick plates. DS15E15T6
164 stands for double-lap with s=1.5d, e=1.5d and 6.35 mm thick plates. S25E30P30T6 stands for
165 single-lap two-bolt in a column with s=2.5d, e=3d, p= 3d and plate thicknesses of 6.35 mm.
166 S30E30G60T3 stands for single-lap two-bolt in a row with s=3d, e=3d, g= 6d and plate
167 thicknesses of 3.175 mm. For all these configurations, ASTM A325 bolts with 12.7 mm
168 diameter and nominal washer on both sides were used. The bolt-hole diameter d_h was
169 approximately equal to 14 mm. Five specimens per configuration were tested except for
170 S30E30G60T3. Three specimens were tested for this configuration for a total of 43 tests.

171 3.2. Experimental setup and measurements

172 The tests were conducted up to failure of the joint in shear using a 500 kN hydraulic testing
173 machine. Figure 2(b) presents the test set-up of aluminum-to-steel connection. The end
174 connections were designed to make the loading axis to coincide with the interface of the two
175 plates so the bolt was primarily loaded in shear. ASTM A325 bolts with 12.7 mm diameter
176 and nominal washer on both sides were used. The length of the bolt was selected to exclude
177 threads from the shear interface. The bolt was tightened to a snug-fit condition, which
178 referred to the maximum effort of a technician using an ordinary wrench. Therefore, the
179 specimen was considered to be bearing type connection. The load was applied at the rate of 1

mm/min and the load and displacement were recorded by the control system of the universal testing machine.

3.3. Tensile tests of the materials

The bolted specimens were taken from different flat bar lots. Flat bars of 63.5 mm and 76.2 mm width had a 6.35 mm thickness; flat bars of 38.1 mm width had three different thicknesses: 3.175 mm, 6.35 mm and 9.525 mm. The flat bar of 152.4 mm width had 3.175 mm thickness. Two or three coupons per flat bars were used to investigate their mechanical properties. For aluminum 6061-T6 flat bars, a total of 19 coupons were prepared and tested in tension according to the American Standard Test Method B 557M-02 (ASTM B557-02) [12]. For the 350W steel flat bars, 12 coupons were prepared and tested in tension according to the American Standard Test Method A370-12 (ASTM A370-12) [13]. All tested coupons had a reduced section. Strain was measured by an axial extensometer with a gage length of 25 mm located at the middle of the reduced section.

4. Experimental results

4.1. Coupons tensile tests results

The mechanical properties of tested aluminum coupons are summarized in Table 2. Stresses were computed from the measured loads data divided by the net-section area of each coupon. The elastic modulus (E) of each coupon was calculated by taking the slope of the elastic portion on its stress-strain curve. Since aluminum does not exhibit a flat plateau at the yield strength as is the case of mild steel, ASTM B 557M-02 [12] suggests to determine the aluminum yield strength ($f_{0.2}$) by the offset method at an offset of 0.2%. As presented in table 2, the strain at maximum tensile stress (ε_{fu}) is approximately 10% while, the strain at $f_{0.2}$ ($\varepsilon_{0.2}$) is between 0.40% and 0.62%. The ultimate tensile strength corresponds to the maximum recorded strength. For coupons $Al_{A\text{-}1}$ and $Al_{B\text{-}2}$, it was difficult to evaluate the yield strain and/or yield strength and the elastic modulus because the acquisition of these curves was

205 faulty. Tensile strength and elastic modulus reported by design references are also presented
206 in Table 2. Commentary in section 4.2.1 of CSA-S157 [3] recommends for design purposes,
207 that f_u and $f_{0.2}$ shall be the minimum value specified for alloy in the Aluminum Standards and
208 Data Publication (ASD) [14]. For aluminum alloy 6061-T6, this minimum corresponds to that
209 of "shapes" which is 260 MPa and 240 MPa for f_u and $f_{0.2}$ respectively. This value is
210 considered regardless if the material is a plate, shape or sheet. Such recommendation is not
211 specified in [1] and [2]. Therefore, f_u and $f_{0.2}$ were taken as provided in Table 3.2a of [1] and
212 Table 7.4.2.1.1 of [2] for aluminum alloy 6061-T6 "plates".
213 For mild steel, yield point is simply the first stress in a material, less than maximum
214 attainable stress, at which an increase in strain occurs without increase in stress [15]. The
215 material's properties of the 5 different lots were similar. The average ultimate tensile strength
216 and average yield strength were approximately 540 MPa and 370 MPa respectively. ASTM
217 A325 bolts were not tested because the strength of the whole connection was not affected by
218 the capacity of the bolt. Its nominal guaranteed tensile strength is 825 MPa and the nominal
219 shear strength for a bolt of 12.7 mm diameter is approximately 63 KN considering the shear
220 strength equals to 0.6 times the nominal tensile strength [15].
221 4.2. Results of bolted connections
222 The average experimental failure loads, P_{exp},. standard deviation, *Std.*, and failure modes,
223 *FM*, for each configuration are presented in Table 3. It can be observed that the average
224 maximum experimental loads for each configuration of single-lap one-bolt joint are
225 approximately 40 kN, 53 kN and 69 kN for S15E15T6, S15E20T6 and S25E25T6
226 respectively. These load values correspond to 63%, 84% and 109% of the nominal capacity of
227 the 12.7 mm A325 bolt in shear which is 63 kN. By increasing the plate thickness to 9.525
228 mm (3/8 in) with e=1.5d and s=1.5d, the average recorded load for S15E15T9 equal 57 kN
229 which is 91% of the nominal capacity of the bolt. For two-bolt joints in a column, the average

experimental failure loads are 95 kN and 120 kN for S25E30P30T6 and S30E30P30T6 respectively. These loads values correspond to 75% and 95% of the nominal capacity of the two bolts. When the two bolts are arranged in one-row, the average failure load is approximately 87 kN for S30E30G60T3 which represent 69% of the nominal capacity of the two bolts.

5. Analysis of experimental results

As all tested configurations did not have the same material tensile strength, the maximum experimental load ($P_{exp.}$) of each tested joint needs to be adjusted for comparison with other test results. For this purpose, the test results were factored by the ratio of the nominal tensile strength required by CSA-S157 [3] design reference ($f_{uCSA\text{-}S157}$ = 260 MPa) to the average tensile strength of the corresponding coupon, $f_{u\ coupon}$ (Equation 1).

$$\text{Factored Load } (P_f) = P_{exp.} \times \frac{f_{u\ CSA-S157}}{f_{u\ coupon}} \quad (1)$$

These factored loads were used to investigate the gain in joint strength between different joint configurations. In Figures 3 to 6, the Factored load was used instead of the experimental load because it allowed to better compare the force-displacement curves for the various configurations.

5.1. Effect of side-distance and end-distance on a one bolt (1X1) single-lap configuration

Figure 3(a) presents the typical failure mode of single-lap aluminum-to-steel one-bolt joints. In this figure, the aluminum plate is on the bottom side while the corresponding steel plate is on the top. The five specimens of each configuration experienced the same failure mode. For S15E15T6, shear tear-out failure of the aluminum plate was observed (Figure 3a). With the increase of the end-distance (S15E20T6), the aluminum plate experienced rupture of the net-section (Figure 3b). A further increase of the end-distance associated with an increase side-distance (S25E25T6) changed the failure mode of the joint to a bearing failure of plate around the bolt-hole in the loading direction (Figure 3c). This elongation, although similar to

255 that of S15E15T6 configuration, was assumed to be bearing failure. This assumption was
256 based on the fact that CSA-S157 [3] recommends that "for force directed towards an edge
257 distance, the capacity is governed by shear failure in the connected material up to an end edge
258 distance in excess of two diameters". With S25E25T6 configuration, a limited yielding of the
259 bolt was also observed. Furthermore, the steel plate reaches its plastic state and an ovalization
260 of the bolt-hole in the steel plate was observed.
261 In Figure 3(d), factored typical force-displacement curves of the three configurations are
262 compared. It is observed that the factored load (P_f) increased by 32% and 61% for S15E20T6
263 and S25E25T6 respectively as compared to S15E15T6. For design consideration, design
264 references such as [1] and [3] suggest to limit the bearing strength of a connection with $e > 2d$
265 to that of approximately $2d$. Experimental results shows that this restriction is acceptable for s
266 lower than $2d$. Above this, such restriction underestimates the bearing strength of a one-bolt
267 connection. An observation of the displacement at which failure occurred in the S15E15T6
268 and S15E20T6 shows that increasing the joint end-distance only did not increase the joint
269 displacement at failure. However, the displacement increased to approximately 10 mm when
270 both the end and side distances were increased to $2.5d$. As S25E25T6 leads to bearing failure
271 and to a higher joint strength, it was taken as a reference baseline for two-bolt connections.
272 5.2. Effect of plate thickness in a one-bolt single-lap configuration
273 The effect of plate thickness was investigated by comparing one-bolt connections with same
274 end and side distances but different plate thicknesses. Figures 4(a), 4(b) and 4(c) present the
275 typical failure mode of specimens S15E15T3, S15E15T6 and S15E15T9 respectively. Results
276 indicate that plate thickness has no effect on the joint failure mode. For this configuration,
277 failure by shear is the observed mode for the three connections.
278 Figure 4(d) presents the typical force-displacement curves of the three tested configurations.
279 The average factored loads of S15E15T3, S15E15T6 and S15E15T9 are 18.8, 33.8 and 47.5

kN respectively. The relationship between the factor load and the plate thickness appears to be not perfectly linear. This effect will be studied further in section 8.1. With S15E15T3, the displacement at failure is approximately 3 mm while with S15E15T6 and S15E15T9 the displacement at failure is around 7 mm.

In Table 3, it can be noted that the factored load obtained with S15E15T9 is only 1.06 times higher than that obtained with S15E20T6 which is 1.5 times thinner but with $e = 2d$. This suggests that a careful selection of the geometric parameters can result in large gains in material weight and cost.

5.3. Effect of joint eccentricity

Joint eccentricity is usually present in single-lap configuration resulting in out-of-plane deformation. Plate end-curling observed as a result of such deformation is more prononced in thinner plates with longer end-distance than shorter ones as illustrated in Figure 5(a) and 5(b). It can be prevented by using an even number of shear planes. The effect of joint eccentricity in the joint axial strength was evaluated by comparing the single-lap S15E15T6 with the double-lap (steel-aluminum-steel) DS15E15T6. In Figures 5(c) and 5(d), failure mode of S15E15T6 is compared to DS15E15T6. As it can be observed, restraining the out-of-plane deformation did not change the failure mode of the joint. Shear tear-out damage is observed on the aluminum plate of both DS15E15T6 and S15E15T6. No significant deformation is observed on the steel plates and on the bolt.

Figure 5(e) presents the force-displacement curves of DS15E15T6 and S15E15T6. A gain of 6% the factored load (P_f) is measured when the eccentricity is restrained. Failure of the DS15E15T6 compared to S15E15T6 occurs earlier in the loading history of the joint. The measured displacement is approximately 5 mm for DS15E15T6 compared to approximately 7 mm for S15E15T6. This is probably due to the two outer steel plates. As their rigididy is 3 times greater than that of aluminum and due to the restriction of out-of-plane deformation,

the ability of the aluminum inner plate to freely deform was reduced. As the strength obtained with the double-lap configuration was only few percent higher than that of single-lap, it was not found necessary to pursue the tests with the double-lap configuration. Therefore, the analysis of the two bolts joint was performed only in single-lap configuration.

5.4. Effect of geometric parameters in two-bolt single-lap configuration

Figures 6(a), 6(b) and 6(c) present the typical failure modes of S25E30P30T6, S30E30P30T6 and S30E30G60T3 respectively. For specimens S25E30P30T6 rupture of the net-section was observed at the aluminum first inner row (Figure 6a). The bolt of the inner row shows sign of shear deformation while the corresponding row on the steel plate shows a light bearing damage. Rupture of the net-section occurs also for S30E30P30T6 on the aluminum first inner row with signs of bearing damage on the two holes (Figure 6b). Signs of bearing damage were also present on the two holes of steel plate while the two bolts reached a plastic state. For S30E30G60T3, failure presented in Figure 6(c) occurs by bearing with hole elongation approximatively equal to 2 times the bolt diameter followed by curling of the aluminum plate. In Figure 6(c), out-of plane deformation of the aluminum plate is observed between the two bolts due to the gage distance, g=6d, taken above the maximum recommended values of EC9 [1] (g=3.5d) and AASHTO [2] (g=4.25d) for a 3.175 mm thick plate. Bearing of the steel plate was also observed while; the two bolts showed signs of damage.

Figure 6(d) presents the typical force-displacement curves of the three configurations. Maximum displacements of 8 mm and 12 mm are observed for S25E30P30T6 and S30E30P30T6 respectively. A gain of 31% of the factored load (P_f) is achieved when the side-distance is increased to 3d. The factored joint capacity in one-bolt connection (S25E25T6) is equal to 54 kN. Doubling the number of bolts with the same side-distance (S25E30P30T6) only increased the joint strength by 46% because the capacity was limited by the rupture of the net-section and the end-distance has no effect on the joint strength. A

further increase of the side-distance to 3*d* (S30E30P30T6) leads to 91% increase in the factored joint strength. As no fracture was observed between the two bolts in both configurations, the pitch-distance *p*=3*d* recommended by [3] is found sufficient to prevent the joint failure on the shear path. Therefore, for the two-bolt in a column with *t*=6.35 mm, a side-distance *s* greater than 3*d* (or $w > 6d$) is required for the joint to achieve the nominal capacity of the two bolts A325 in shear. This value of *s* is expected to change with the plate thickness, the number of bolt in the joint, and the bolt size and properties.

Figure 7(d) also shows the force-displacement curve for specimen S30E30G60T3. The results of this specimen will be used later to validate the FE model for the two-bolt in a row configuration.

6. Comparison between experimental and predicted results

The test results of one-bolt and two-bolt connections are compared with the nominal strength prediction obtained using equations recommended by [1], [2] and [3]. As only the nominal strength is considered, strength reduction factors are not used for the calculation of the strength predictions.

6.1. Design Equations

When failure is predicted to occur in the net-section, all three design references establish the corresponding net-section strength (T_r) presented in Equation 2.

$$\text{Nominal net} - \text{section strength } (T_r) = (w - nd_h)tf_u \quad (2)$$

The three design references do not give a clear guideline of the shear tear-out strength (S_r) prediction as it is the case of steel structures. As shear tear-out is a particular case of block shear failure also called tear-out in [3], it was assumed that block-shear strength equation in these design references can also be applied to shear tear-out strength. Therefore, the nominal shear-tear-out strength per bolt was evaluated using Equations 3 to 5.

$$\text{CSA} - \text{S157 [3] nominal Shear tear} - \text{out strength } (S_r) = etf_u \quad (3)$$

EC9 [1] nominal Shear tear − out strength $(S_r) = 0.58(2e - 0.5d)tf_u$ (4)

AASHTO [2] nominal shear tear − out strength $(S_r) = 1.16etf_u$ (5)

The nominal bearing strength (B_r) per bolt is evaluated using Equation (6) to (8) for [3], [1] and [2] respectively. It can be seen in Equation (8) that the bearing strength of the material is required to evaluate the connection bearing strength. This strength was not evaluated for the coupons tested in this study. Therefore, the ratios of f_{bu}/f_u and f_{by}/f_y calculated from values provided in [2] design reference Table 7.4.2.1 were used. From the values provided in this reference, the bearing strength of aluminum alloy 6061-T6 (f_{bu}) equals $2.1f_u$ while the bearing yield strength (f_{by}) equals $1.66f_y$. These ratios were used in conjunction with the coupon tensile strength as presented in Equation 8. For $e<2d$, AASHTO [2] recommends to multiply B_r by the ratio of $e/2d$

$$\text{CSA} - \text{S157 [3] nominal bearing strength } (B_r) = \min\begin{cases} etf_u \\ 2dtf_u \end{cases} \quad (6)$$

$$\text{EC9 [1] nominal bearing strength } (B_r) = 2.5\alpha_b df_u \text{ with } \alpha_b = \min\begin{cases} \frac{e}{3d_h}, \\ 1, \\ \frac{f_{ub}}{f_u} \end{cases} \quad (7)$$

$$\text{AASHTO [2] nominal bearing strength } (B_r) = \min\begin{cases} dtf_{by} = 1.66dtf_y \\ dtf_{bu}/1.2 = 1.75dtf_u \end{cases} \quad (8)$$

6.2. Analysis of the predicted results

Table 3 column 5 to 13 lists the predicted failure modes and failure loads of the three design references. The material tensile strengths obtained from the tested coupons were used for this calculation. Therefore, the predicted load P_n should be compared to the predicted experimental load P_{exp}. The experimental to predicted ratios are also reported in Table 3.

For connections S15E20T6, S25E30P30T6 and S30E30P30T6, experimental study reveals a failure mode by net-section. However, with EC9 [1] and AASHTO [2] bearing strength was found to govern the design prediction of these three configurations. Failure prediction by CSA-S157 [3] was consistent with the experimental failure for S15E20T6 and S25E30P30T6.

However bearing strength governs the design prediction for S30E30P30T6. With [3], the net-section capacity was also well predicted with a maximum difference of 14% compared to experimental failure load. The strength of these connections was underestimated by 20% to 64% compared to experimental results when bearing failure was the predicted mode.

For connections S15E15T3, S15E15T6, S15E15T9 and DS15E20T6, it was assumed in the experimental analysis that the observed failure mode is shear tear-out (instead of bearing) because of $e < 2d$ as suggested in [3]. However, with [1] and [2] design predictions, bearing strength was found to govern the design prediction. Failure prediction by [3] was consistent with the experimental failure as the shear strength equation (Equation 3) is equal to the lower bound of bearing strength (Equation 6). With [1] and [2], the predicted strength was found to be very conservative with a maximum difference of 60% compared to experimental results. As for [3], a better prediction of the strength was obtained with a maximum difference of 20% compared to experimental results.

For connections S25E25T6 and S30E30G60T3, all three design references predicted a bearing failure which is consistent with the experimental failure mode. However, the bearing strength prediction of these three references underestimated the connection strength by 30% to 106% as compared to experimental results. This is due to the fact that design references limit the bearing strength to approximately twice the ultimate tensile strength. For $e>2d$, such limitation underestimates the connection strength.

More data are required to better comprehend the relationship between different geometric parameters and the joint strength and to develop design equations capable of providing an accurate prediction of the joint strengths. Finite element analysis is a good tool to extend such data.

7. Finite element analysis

7.1. Overview of the finite element model

A finite element (FE) analysis was performed to investigate the strength of aluminum bolted joints with the commercial software ADINA 8.7.3. The analysis started with a validation study. The experimental results were used to validate the FE results. This analysis was followed by a parametric study where a 3D FE analysis was used to study the effect of plate thickness and verify the assumption made in section "Effect of plate thickness". For this verification, t=3.175 mm, 6.35 mm, 9.525 mm, 12.7 mm, 15.875 mm, 19.05 mm, 25.4 mm with the constant values of e=1.5d and s=1.5d were considered. Then, the effects of increasing the end-distance (e= *1.5*d, 2d, 3d, 4d, 5d) and the side-distance (s=1.5d, 2d, *2.5*d, 3d, 4d, 5d) in one-bolt connection were analyzed using 2D FE analysis. Finally, the optimum geometric parameters for two-bolt connections either aligned parallel or transversal to the loading direction were investigated. The end-distance and the side-distance were varied from 1.5d to 5d as in one-bolt configuration while increasing the pitch-distance (p=2d, 3d, 4d, 5d) for two-bolt parallel or the gage-distance (g=2d, 3d, 4d, 5d) for two-bolt transversal to the loading direction were considered. In line with the experimental investigation, maximum geometric parameters beyond which there is no increase in the joint strength were evaluated. Results obtained from this analysis were also used to evaluate the optimum parameters of one and two bolts connection for different plate thicknesses, bolt sizes and bolt grades. A linear relationship between the joint strength and both the plate thickness and bolt size was assumed. These optimums were chosen based on the values at which the nominal shear strength of a high strength bolt A307, A325 and A490 is reached. The recommendation of AASHTO [2] to limit the net-area (A_n) of the connecting element to the maximum value of 85% the gross-area (A_g) of the plate was also taken in consideration. Although such requirement is not specified for aluminum structures, it was considered for choosing the side and gage distances to make sure an economic design is identified.

7.2 Analysis assumptions

In the experimental study of the aluminium-to-steel connection, failure of the joint was due to the aluminum fracture. Therefore, to reduce the computation time, only the aluminum plate and bolt were modeled in the finite element (FE) analysis. To ensure that the model reliability will not be affected with such simplification, a 3D model, which includes the aluminum plate, the steel plate and the bolt (FE_3DAS) was also computed. The results obtained with the 2D (FE_2DA) and 3D (FE_3DA) simplified models were compared to FE_3DAS and experimental results. As bolts were tightening to a snug-fit condition (bearing type connection), the bolt preload was neglected. The bolt preload was also not considered in the FE analysis by [10] for the same preload condition. Figures 7(a) and 7(b) present the typical FE_3DAS and FE_3DA models used for this analysis.

For model validation, all configurations tested in the experimental program were analysed. Material properties of these configurations are shown in Table 2. In the static environment of ADINA, the aluminum and steel plates were modeled as a material with bilinear elasto-plastic behavior. The 3D solid element with 8 nodes per element and 3 degrees of freedom was considered. The analysis assumptions were large displacement and strain. Full Newton method was used for the iteration. The bolt was modeled as a cylinder of 12.7 mm diameter. Contacts between the bolt and the plates were modeled by contact elements available in the FE software. The contact interface were generated as a pair of surface elements. On this interface, a bolt was defined as a target surface and the bolt-hole as a contactor surface. This assumption was based on the fact that the strength of the steel bolt is greater than that of aluminum and steel plates. No friction was considered on this interface. For the 3D model containing the steel and aluminum plates (3DAS), fixed boundary condition was applied on the aluminum far end plate edge (X=Y=Z=0) and a uniform pressure was applied in the longitudinal z axis of the far end plate edge of the steel plate (Figure 7a). For the 3D simplified model containing only the aluminum plate (3DA), fixed boundary condition was

applied on the bolt (X=Y=Z=0) and a uniform pressure was applied in the longitudinal z axis of the far end plate edge of the aluminum plate (Figure 7b). The external load was incrementally applied on the structure. Once the deformation of the material at f_u (ε_{fu}) was reached, the structure diverged. The load to which the structure diverged was taken as the maximum capacity that the joint can support.

For the parametric study, $f_{0.2}$=279 MPa, f_u=310 MPa, $\varepsilon_{0.2}$=0.4% and ε_{fu} =10% were considered. A 3D FE analysis was first used to investigate the effect of plate thickness. Then, to further reduce the computational process, a 2D FE analysis was considered to evaluate the effects of *e*, *s*, *p* and *g*. In addition to the FE modeling assumptions described above, six degrees of freedom and 9 nodes per element were used for 2D FE model (2DA). The bolt was modeled as a half cylinder and the contact feature available in the software was used. The parameters: *e*, *s*, *p* and *g* were consecutively changed while *d*=12.7 mm and the input plate thickness (*t*=6.35 mm) were kept constant.

7.3 Model validation

Figure 7(c) to 7(e) present the post-processing strain distribution of the FE model. Based on the plastic strain distribution along a given failure path of the model, the joint failure mode was defined. For example, for net-section failure, plastic strains are developed across the centerline of the bolt-hole in the net-section path (Figure 7c). For shear tear-out failure presented in Figure 7(d) plastic strains are developed between the side of the bolt-hole up to the free end edge of the plate while in bearing failure presented in Figure 7(e), plastic strains are limited ahead of the bolt hole in the bearing path and barely reach the free end edge of the plate.

In Figure 8, the typical force displacement curves obtained in the FE analysis are compared to that of experimental results. In general, no significant difference in the failure loads are observed between the three different models. In Figure 8(a) and 8(b) it can be observed that

the elastic portion of the force-displacement history of FE_3DAS is stiffer than that of FE_3DA and FE_2DA. On the other hand, it can be observed that the curves of FE_3DA and FE_2DA in Figure 8(a) to 8(d) are quite consistent with that of experimental results up to the peak load at which the FE models stop. Therefore, the simplified 2D (FE_2DA) and 3D (FE_3DA) models will be used for the rest of the study.

In Table 4, the ultimate loads and failure modes obtained from simplified 2D and 3D FE analyses of one and two bolts connections are compared to the average failure loads obtained in the experimental analysis. As it can be observed, both 2D and 3D results are in good agreement with experimental results, FE failure loads are mostly conservative. The ratios of experimental to predicted results are within 11% difference for 3D and 2D models. The observed FE failure modes were also consistent with the experimental failure mode. Therefore, the 3D and 2D models are enough reliable to be used for the parametric analysis.

8. Parametric simulation and analysis of the results

Following the satisfactory agreement between 2D, 3D FE models and experimental results, a parametric study was carried out. The results obtained from the parametric simulation are presented in Figure 10, Tables 5 and 6.

8.1. Effect of plate thickness in one-bolt connection

The effect of plate thickness on the joint strength were analysed by keeping the material properties ($f_{0.2}$=279 MPa, f_u=310 MPa, $\varepsilon_{0.2}$=0.4% and ε_{fu} =10%) and e=s=1.5d constant with varying values of t (t=3.175 mm, 6.35 mm, 9.525 mm, 12.7 mm, 15.875 mm, 19.05 mm, 25.4 mm). Results obtained from this simulation are presented in Figure 9. Figure 9(a) shows the plastic strain distributions of S15E15T25, S15E15T12 and S15E15T3. Failure occurs by shear tear-out regardless of the size of the plate thickness. In Figure 9(b), it can be observed that the relationship between the plate thickness and the joint strength is to a certain extent linear in the model. The experimental results obtained for S15E15T3, S15E15T6 and

S15E15T9 are also presented in this figure. It was observed experimentally that the relationship between the plate thickness and the average joint strength was not perfectly linear. However, by tracing all the data obtained experimentally for these configurations in Figure 9(b), the linear relationship between the plate thickness and the joint strength is an acceptable simplification. The possible non-linearity of this relationship would need to be studied with additional experimental tests. In particular, for plates with large thicknesses, which are realistic in the context of bridge construction, no experimental data was found in the literature and therefore the numerical results proposed in this study would need to be further studied with experimental tests to confirm the trends observed.

For the evaluation of the optimum parameter, the linear relationship between the bolt diameter and the plate thickness was assumed as demonstrated by the experimental study of Wang et *al*. [6] and section 8.1. Results obtained from the FE analysis and presented in Table 5 and 6 were used to extrapolate the strength of connections with different plate thicknesses and bolt diameters. Tables 7 to 9 present the proposed optimum for values of 6.35 mm$\leq t \leq$ 25.4 mm and 12.7 mm$\leq d \leq$25.4 mm. In these tables, cells with no value are those from which the plate thickness could not sustain the capacity of the bolts or which required a side-distance larger than the maximum recommended values of both [1] and [2] and from which the ratio of $A_n/A_g > 0.85$. The following paragraphs described some of the important results obtained in the parametric simulation and the criteria behind the choice of optimum parameters.

8.2. Optimum end-distance (*e)* and side-distance (*s)* in one-bolt connection

Figure 10(a) presents the effects of the end-distance (on the positive x-axis) and the side-distance (on the negative x-axis) on the failure load for one-bolt joint as obtained by the FE analysis for t=6.35 mm and d=12.7 mm. The predicted strengths of the one-bolt joint using the maximum and minimum e and s recommended by EC9 [1] were also evaluated and are

528 presented in this figure. These minimum are equal to 1.2d for s and e while the maximum is
529 4t+40 mm for both s and e which corresponds to 5.15d for t=6.35 mm and d=12.7 mm. FE
530 results show an increase of the joint capacity with the increase of s and e up to a limit value
531 of 3d and 4d respectively. Table 5 shows the FE results of one-bolt connection. It can be
532 observed that the strength of the connection is governed by net-section failure at $s < e$, shear
533 tear-out failure for $e \leq s \leq 2d$ and bearing failure for e and $s > 2d$. Comparisons between the
534 strength obtained from FE analysis at the limits of 3d and 4d for s and e respectively reveals
535 that the measured gain is 33% and 75% higher than the predicted strength at maximum and
536 minimum values recommended by [1]. These values are consistent with the maximum values
537 recommended by [1], which are 5.15d (4t+40 mm) for both s and e. For design consideration,
538 design references such as [3] suggest to limit the bearing strength of a connection with $e > 2d$
539 to that of 2d. Figure 10(a) shows that this restriction is acceptable for s lower than 2d. Above
540 this, such restriction underestimates the bearing strength of a one-bolt connection. From
541 Table 5, the values of s=2d and e=3d were found sufficient to improve the connection
542 strength to that of one bolt A325 nominal shear strength with d=12.7 mm and t=6.35 mm.
543 With the value of s =2d, the ratio of A_n/A_g = 0.75 which is lower than the limit ratio of 0.85 is
544 obtained. The optimum parameters of one-bolt with varying bolt sizes, plate thickness and
545 bolt grade are presented in Table 7. It can be observed that optimum values are related to the
546 bolt diameters, bolt grade and plate thickness. For bigger bolt size (d=25.4 mm) or A490 bolt
547 grade, these optimums can reach the limit of 3d and 4d for s and e respectively with A_n/A_g
548 <0.85.

549 8.3. Evaluation of the optimum geometric parameters for two-bolt joint in a column

550 Figure 10(b) presents the effects of geometric parameters for the joint with two bolts parallel
551 to the loading direction, as obtained from the FE analysis for t=6.35 mm and d=12.7 mm. The
552 predicted strengths of the two-bolt joint using the maximum and minimum e, s and g

553 recommended by [1] are also presented. The maximum and minimum *e* and *s* are the same as
554 in one-bolt joint while the limit values of *p* are: $2.4d \leq p \leq 7d$ ($14t$). On the positive x-axis of
555 Figure 10(b), the effect of *e* with *s*=1.5*d*, 3*d* and 4*d* and varying pitch (*p*=2*d* to 5*d*) is
556 depicted. Except for $s \geq 4d$, it can be observed that at $e \geq 2d$, *e* has a negligible effect on the
557 joint strength. This value of 2*d* is consistent with the minimum limit of *e* recommended by
558 [2]. For a constant value of *s*, the observed increase in strength is related to the increase of the
559 pitch-distance up to *p*=3*d*. Above this value, the plateau indicates that with the increase of *e*
560 and *p*, the joint strength continues to increase with *s*. This last effect is represented on the
561 negative x-axis for a constant value of *e*=3*d*. It is shown that the increase of the joint strength
562 is consistent with the increase of the side-distance. From *s*=1.5*d* to 3*d*, *p* has no effect on the
563 joint strength. This is because the net-section strength governs this value as shown in Table 6
564 for 1X2 configuration. Above *s*=3*d*, the effect of *p* becomes evident while *s* remains the main
565 parameter affecting the joint strength. FE results presented in Table 6 for 1X2 configuration
566 reveal that the failure mode occurs by bearing for *s*>3*d*. The effect of (*e*) on the joint strength
567 as calculated with [1] shows that limiting the value of *s* to the minimum values (*s*=1.5*d*) will
568 limit the strength of the two-bolt joint in a column to that of one-bolt joint with similar width.
569 Similar interpretation can be obtained from FE results. For example in Table 5 for *s*=1.5*d*,
570 *e*=2*d*, the load of one-bolt connection is equal to 47.8 kN. In Table 6, for two-bolt in a
571 column, *s*=1.5*d*, *p*=3*d*, failure load is equal to 48.4 kN. Therefore, the choice of *s* should be
572 consistent with the number of bolts in the column and the plate gross area (A_g). For this
573 configuration, *s*=3*d* was found sufficient to improve the joint strength to the nominal capacity
574 of the two bolts in shear. This value is lower than the maximum limit recommended by [1],
575 although 9% higher than that of [2]. On the other hand, the ratio of $A_n/A_g = 0.82 < 0.85$ is
576 obtained. With this choice of *s*, the values of *p* and *e* can therefore be limited to 3*d* and 2*d*
577 respectively for *t*=6.35 mm and *d*=12.7 mm. The optimum parameters of two-bolt in a

column with varying bolt sizes, plate thickness and bolt grade are presented in Table 8. The optimum value of s is found to vary with the plate thickness and the strength of the bolts and should be limited to 4d although at this value, $A_n/A_g = 0.86$.

8.4. Evaluation of the optimum geometric parameters for two-bolt joint in a row

Figure 10(c) presents the effects of joint parameters for two-bolt in a row, as obtained from the FE analysis for t=6.35 mm and d=12.7 mm. The predicted strengths of the two-bolt joint using the limit values recommended by [1] are also presented. These limit values of g are $2.4d \leq g \leq 7d$ (14t). The effect of e presented on the positive x-axis is evaluated by considering a 3d side-distance with varying end-distance (e=1.5d to 5d) and gage-distance (g=2d to 5d). It can be observed that both g and e have an effect on the joint strength. The effect of e becomes negligible at 4d with $g>3d$ while the joint strength continues to increase with the gage-distance. The effect of s with a constant e=3d, varying side-distance (s=1.5d to 5d) and gage-distance (g=2d to 5d) is shown on the negative x-axis of Figure 10(c). It can be observed that the joint strength increases with s up to 3d while it continues to increase with g. At minimum recommended values of s and g, the predicted strength of the connection is governed by net-section failure. At maximum recommended values, bearing is the predicted failure mode. FE results presented in Table 6 for 2X1 configuration show that block-shear and bearing are the observed failure modes for $s \geq 2d$ while net-section failure is observed with narrow side-distance (s=1.5d) and shear tear-out failure for short end-distance (e=1.5d). With e=3d, limiting s and g to the minimum values recommended by [1] (s=1.2d and g=2.4d) limits the predicted nominal strength to that of the one-bolt joint with similar width. However, with the same end-distance, increasing s to 3d and simultaneously considering g=3d improve the predicted nominal strength to that of the two bolts (A325). With these values, the ratio of $A_n/A_g = 0.78$ which is lower than the limit of 0.85 is obtained. From values reported in Table 6 and the above analysis, e=3d, s=3d and g=3d are proposed for d=12.7 mm

and t=6.35 mm. The proposed values are between the limits recommended by [1] although e and s are 9% above the maximum recommended by [2]. The optimum parameters of two-bolt in a row with varying bolt size, plate thickness and bolt grade are presented in Table 9. It is shown that for s=3d, the proposed optimums can reach the limit of g=5d and e=3d. However, for this value of g, the A_n/A_g = 0.82.

9. Conclusion

The aim of this study was to critically examine the recommendations of three design references namely EC9 [1], AASHTO [2] and CSA-S157 [3], to evaluate the maximum geometric parameters beyond which no major increase of joint strength is observed and to propose optimum geometric parameters for one-bolt and two-bolt connections. The chosen optimum was based on the values at which the shear strength of the three grades of bolt (A307, A325, and A490) is reached and on the limit of $A_n \leq 0.85A_g$. It was found that the joint geometric parameters have a high impact on the load performance and failure mode. In summary:

- For one-bolt configuration, experimental analysis on aluminum-to-steel connections shows that to achieve bearing failure, e and s should not be less than 2.5d. Above this, bearing damage was observed on steel plate and on the bolt. It was shown from the finite element analysis that maximizing the geometric parameters can result in an increase of the joint strength of more than 75% compared to the minimum values recommended by the design references. Although maximum e and s was observed at 4d and 3d respectively, the optimum values were found to be related to the bolt diameter, bolt grade and plate thickness. The proposed optimum were within the limit of EC9 [1] and/or AASHTO [2] recommended values and the ratio of A_n/A_g <0.85.
- For two-bolt connections in a column, it was observed from the experimental study that pure bearing failure is not likely to occur. The pitch p=3d was found sufficient to

sustain the joint and prevent the failure between the holes. Finite element analysis indicates that the side-distance is the main parameter that controls the strength of the connection. Limiting the side-distance to the minimum recommended value s=1.5d was found to limit the strength of two bolts in a column to that of the one bolt connection. The effect of p was evident after $3d$ while e>2d was found to have limited effect on the joint strength. For this configuration, the proposed optimum parameters should be taken at e=2d, p=3d while s varies with the plate thickness and the nominal shear strength of the bolts and should be limited to 4d although at this value, A_n/A_g = 0.86.

- For the configuration with two-bolt in a row, the strength of the connection was found to increase with s and e up to the limit value of 3d and 4d respectively. The increase of the joint strength was consistent with the increase of g. With the proposed optimum, the strength of connection reached the nominal shear strength of the bolts and the ratio of A_n/A_g was less than 0.85.

- Compared to double-lap connection, the effect of the out-of-plane deformation observed experimentally in the single-lap configuration with s=1.5d and e=1.5d did not change the failure mode of the aluminum specimen. However, restraining the joint eccentricity with a double-lap configuration was found to slightly improve the joint strength. Out-of-plane deformation was more pronounced in connection with long end-distance and thinner plate.

- Predicted failure modes were not always consistent with experimental failure mode. In most cases, bearing was found to govern the strength of the connections. The calculated bearing strengths were found to underestimate significantly the connection strength. Compared to EC9 [1] and AASHTO [2], CSA-S157 [3] was found to provide a better prediction of the failure mode and failure load of the connections.

653 **ACKNOWLEDGEMENTS**

654 The financial support provided by Natural Science and Engineering Research Council of
655 Canada (NSERC) and Centre québecois de recherche et de développement de l'aluminium
656 (CQRDA) is acknowledged.

657

658 **REFERENCES**

659 [1] EC9. (2007). "Eurocode 9: Design of aluminum structures". European Committee for
660 Standardization, Brussels.
661 [2] AASHTO (2010). "AASHTO LRFD Bridge Design Specifications", *American*
662 *Association of State Highway and Transportation Officials*, 5th edition.
663 [3] CSA-S157 (2007). "Strength Design in Aluminum/Commentary on CSA S157-05,
664 Strength design in aluminum". Canadian Standards Association.
665 [4] Menzemer, C.C., Fei, L., Srivastsan, T.S. (1999). "Design Criteria for Bolted connection
666 elements in aluminum alloys 6061", *Journal of Mechanical Design*, Vol. 121, p. 348-358.
667 [5] Menzemmer, C.C., Ortiz-Morgado, R. and Iascone, R. (2002). "An investigation of
668 bearing strength of three aluminum alloys", *Materials Science and Engineering A327*, p. 203-
669 212.
670 [6] Wang, Y., Yuan, H., Shi Y., Zhang, G. (2011). "Bearing Performance and design method
671 of aluminum alloy bolted connections", *Applied Mechanics and Materials*, Vols. 71-78, p.
672 882-889.
673 [7] Kim, T., Jo Y.H., Kim, S. and Lee, Y.T. (2012). "Ultimate Behavior of Single Shear
674 Bolted Connections with Thin-walled Aluminum Alloys (6061-T6)", *Advanced Materials*
675 *Research*, Vols. 446-449, p. 3441-3445.
676 [8] AISI S100 (2007). "American Iron and Steel Institute". *North American Specification for*
677 *the Design of Cold-Formed Steel Structural Members*.
678 [9] ADM. (2010). "Aluminum Design Manual". The Aluminum Association, Washington,
679 D.C.
680 [10] Kim, T., Jo Y.H. and Choi, Y.C. (2012). "Numerical Investigation on Structural
681 Behavior and Curling influence of aluminum alloy bolted Connections", *Applied Mechanics*
682 *and Materials*, Vols. 166-169, p. 885-889.
683 [11] Tinl, N., Menzemer, C.C., Manigandan, K. and Srivatsan, T.S. (2013). "The Bearing
684 Strength and Fracture Behavior of Bolted Connectionns in Two Aluminum Alloys", *Journal*

of Materials Engineering and Performance, ASM International, DOI: 10.1007/s11665-013-0643-7.

[12] ASTM B557-02 (2002). "Tension testing wrought and cast aluminum and magnesium—Alloy products", *ASTM International*, Conshohocken, PA.

[13] ASTM A370-12 (2012). "Standard Test Methods and Definitions for Mechanical Testing of steel Products", *ASTM International*, West Conshohocken, PA.

[14] ASD (2003). "Aluminum Standards and Data", The Aluminum Association, Inc.,Washington, DC.

[15] Kulak, G. L., Adams, P.F., Gilmor, M.I. (1998). "Limit States Design in Structural Steel" *Canadian Institute of Steel Construction*, 5th edition.

List of Figures

723 **List of Tables**

733

734

735

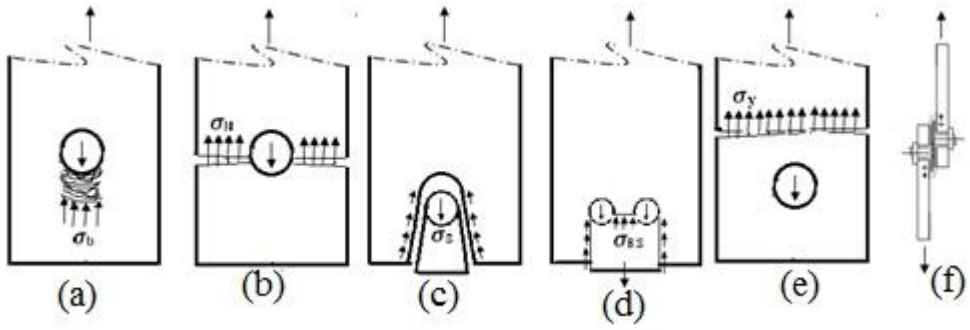

736 Figure 1. Failure modes: (a) Bearing, (b) net-section, (c) shear tear-out, (d) block-

737

738

739

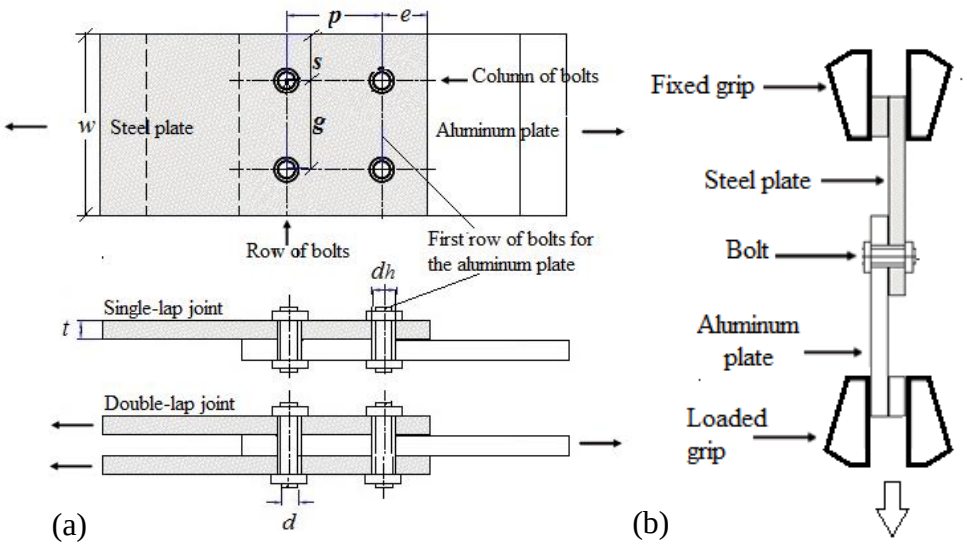

Figure 2. (a) Typical bolted joint in single-lap and double-lap arrangements, (b) Test set-up of aluminum to steel connection

740

741

742

743

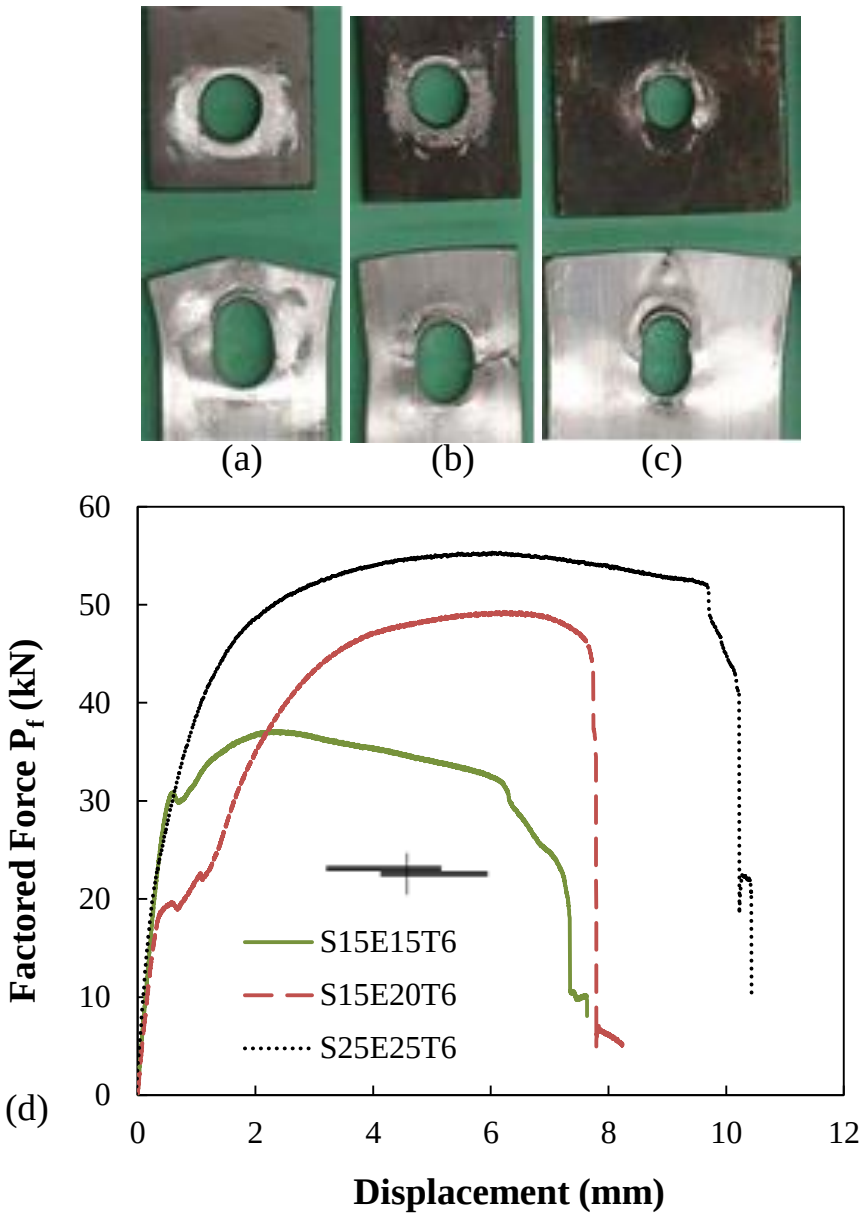

Figure 3. Effect of *s* and *e* on one bolt single-lap joints: Damage on: (a) S15E15T6, (b) S15E20T6, (c) S25E25T6, (d) Factored Force-Displacement curves of one bolt single-lap joints.

744

745

746

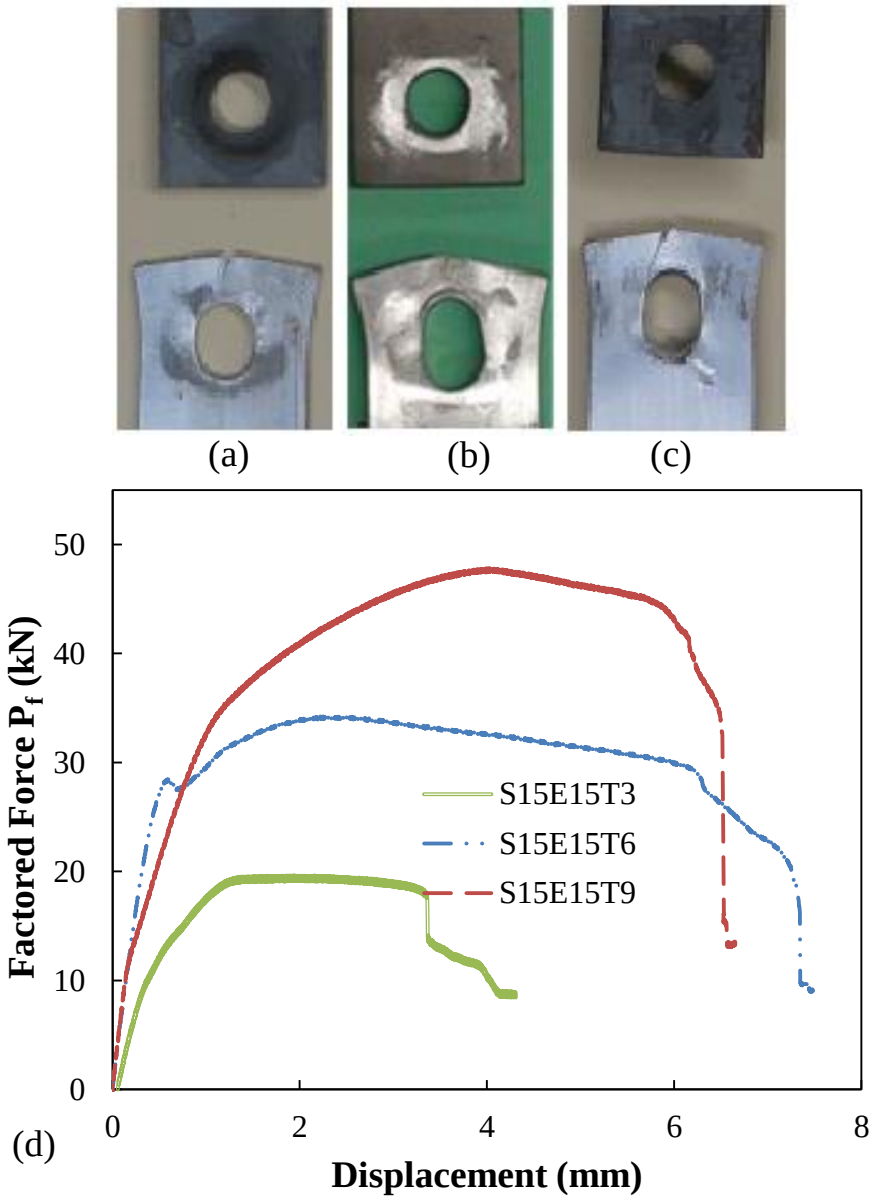

Figure 4. Effect of plate thickness on one bolt single-lap joints: Damage on: (a) S15E15T3; (b) S15E15T6; (c) S15E15T9, (d) Factored Force-Displacement curves

747

748

749

750

751

752

753

754

755

756

757

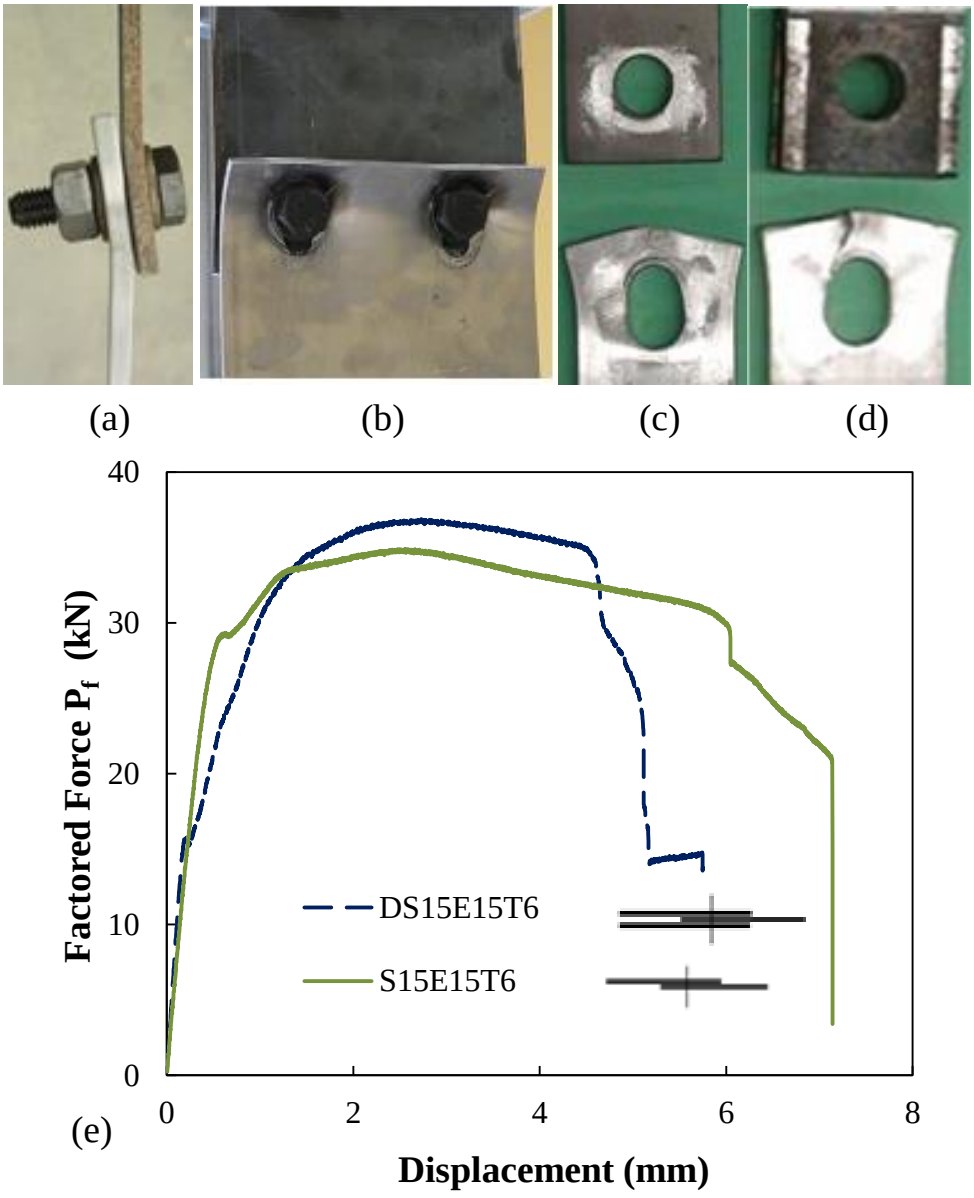

Figure 5. Effect of joint eccentricity: Out-of-plane deformation of (a) S15E15T6 and (b) S30E30G60T3. (c) Fracture of S15E15T6, (d) Fracture of DS15E15T6, (e) Factored force-displacement curves of DS15E15T6 compared to S15E15T6

758

759

760

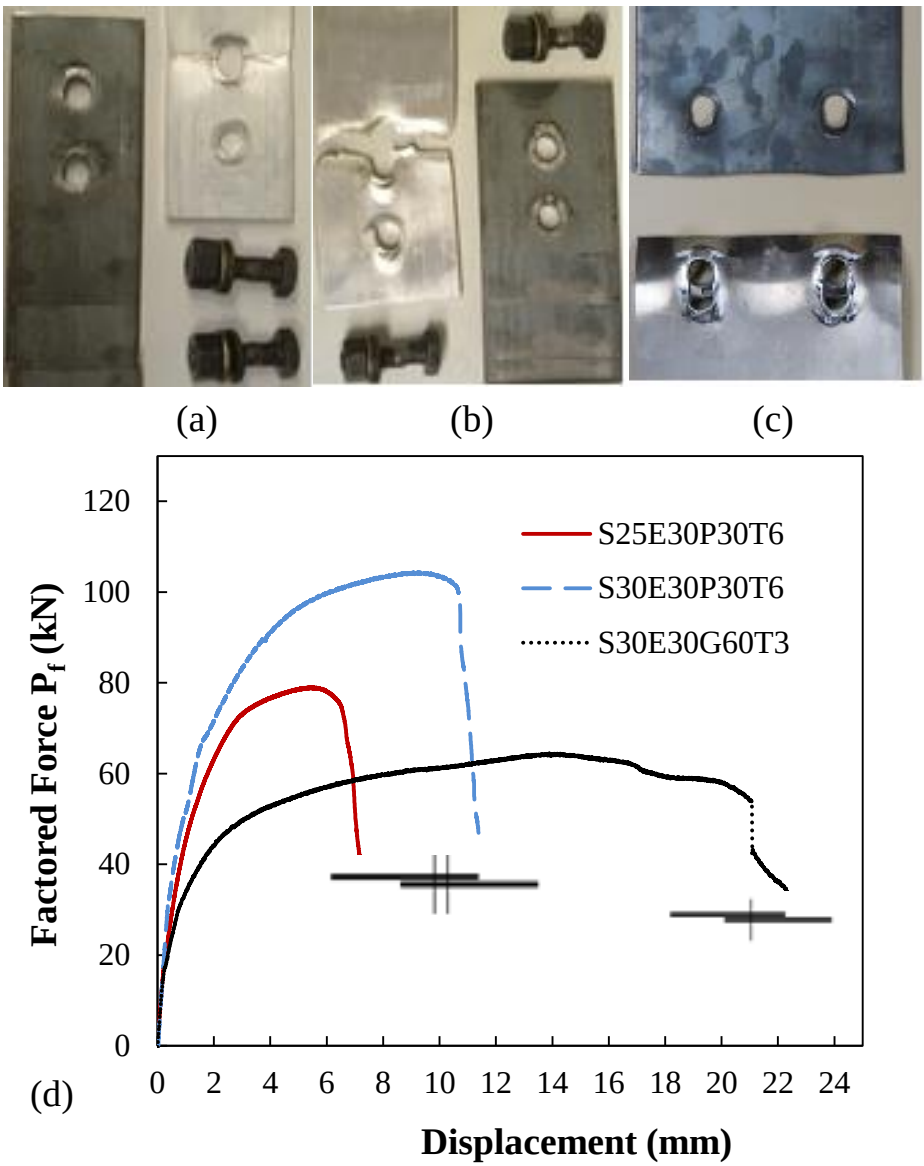

Figure 6. Effect of geometrical parameters in two-bolt single-lap configuration: Damages on 2 bolts joints: (a) S25E30P30T6; (b) S303E0P30T6; (c) S30E30G60T3, (d) Factored force-displacement curves of S30E30P30T6, S25E30P30T6 and S30E30G60T3

761

762

763

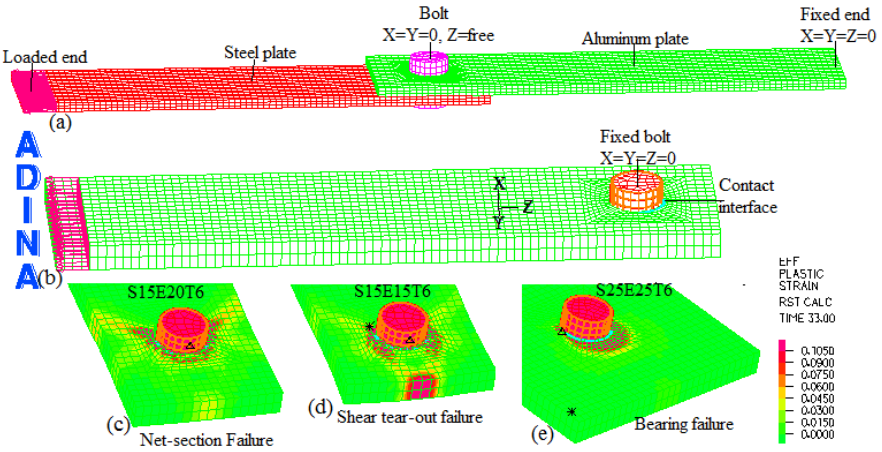

Figure 7. FE models: (a) Typical FE_3DAS model, (b) Typical FE_3DA model. Post-processing response: (c) Net-section failure, (d) Shear tear-out failure, (e) Bearing failure

764

765

766

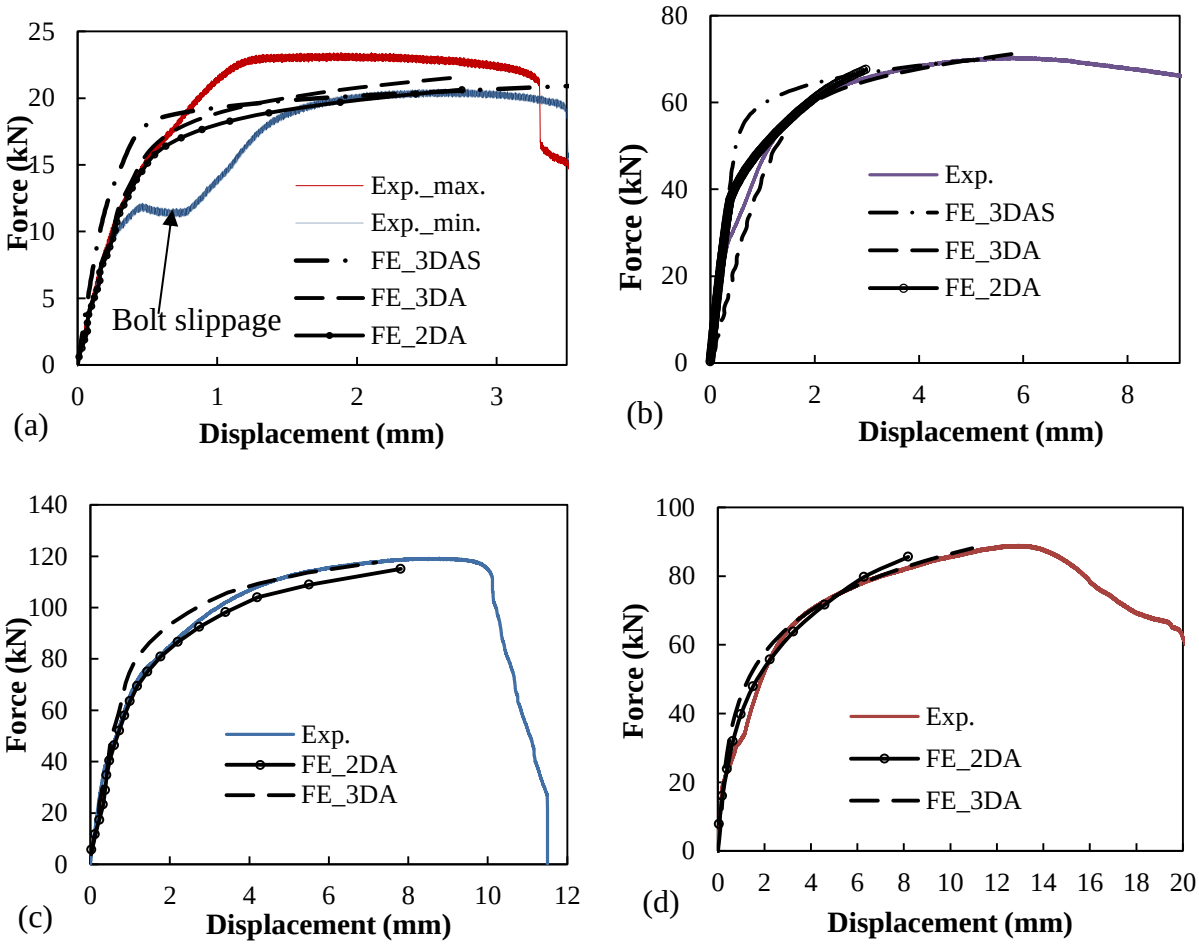

Figure 8. Typical force-displacement curves of the experimental compared to finite element models: (a) S15E15T3, (b) S25E25T6, (c) S30E30P30T6, (d) S30E30G60T3

767
768

769

770

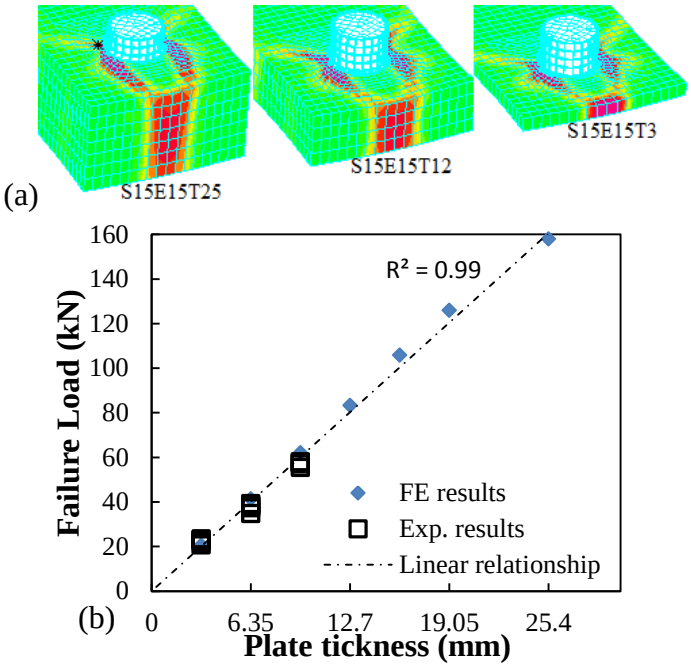

Figure 9. Effect of plate thickness on the joint strength: (a) failure modes, (b) Relationship Failure Load-Plate thickness

771

772

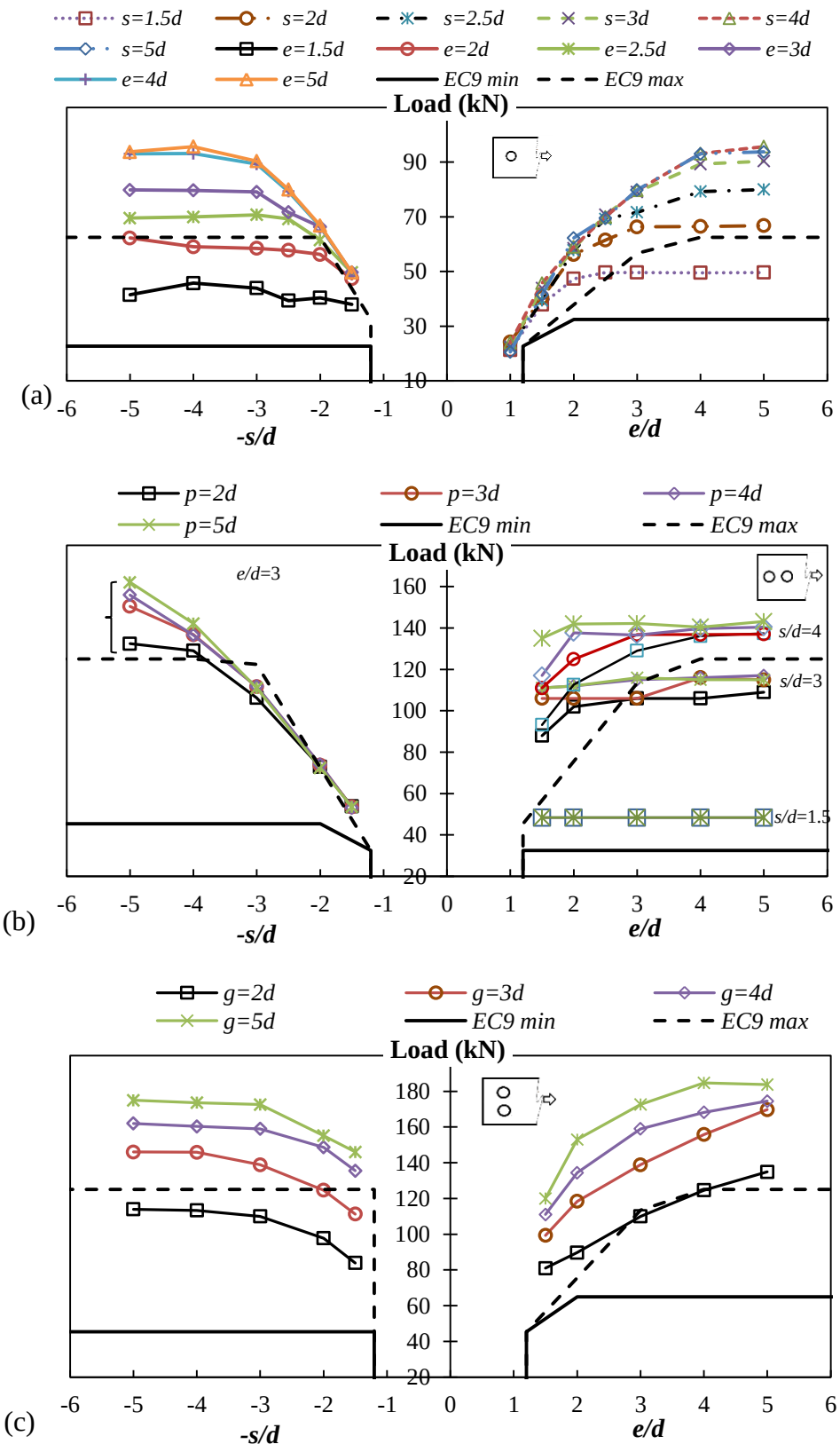

Figure 10. Effect of (a) end-distance and side-distance on one bolt, (b) end-distance and side-distance on 2-bolt in a column, (c) end-distance and side-distance on 2-bolt in a row

774

775

776 Table 1. Geometric recommendations for aluminum bolted connection

Design Codes	**Pitch (*p*)**		**Gage (*g*)**		**End-distance (*e*)**		**Side-distance (*s*)**	
	Min.	**Max.**	**Min.**	**Max.**	**Min.**	**Max.**	**Min.**	**Max.**
CSA-S157 [3]	3*d*	-	2.5*d*	-	1.5*d*	-	1.25*d*	-
AASHTO [2]	2.5*d*	17*t*	2.5*d*	17*t*	$2d_h$	5.5*t* or 90 mm	$1.5d_h$	5.5*t* or 90 mm
EC9 [1]	2.2*d*	14*t* or 200 mm	2.4*d*	14*t* or 200 mm	1.2*d*	4*t* + 40mm	1.2*d*	4*t* + 40mm

777

778
779

780 Table 2. Aluminum tensile test results (coupons)

Corresponding bolted specimens	Couponname	f_u (MPa)	$f_{0.2}$ (MPa)	ε_{fu} (%)	$\varepsilon_{0.2}$ (%)	E (GPa)
Al-St S15E15T3	Al_{A_1}	310.4	280.5	-	0.54	78.4
	Al_{A_2}	309.1	277.5	7.7	0.52	69.3
	Al_{A_3}	310.2	279.6	9.6	0.53	67.5
	Aver.	*309.9*	*279.2*	*8.7*	*0.53*	*71.7*
Al-St S15E15T6	Al_{B_1}	305.1	279.0	8.0	0.43	69.4
	Al_{B_2}	300.1	-	-	-	-
	Aver.	*302.6*	-	-	-	-
Al-St S15E15T9	Al_{C_1}	312.2	293.3	7.8	0.62	64.7
	Al_{C_2}	313.7	294.3	8.0	0.6	70.9
	Al_{C_3}	311.3	292.9	7.8	0.61	73.0
	Aver.	*312.4*	*293.5*	*7.9*	*0.61*	*69.5*
Al-St S15E20T6	Al_{B_1}	305.1	279.0	8.0	0.43	69.4
	Al_{B_2}	300.1	-	-	-	-
	Aver.	*302.6*	-	-	-	-
Al-St S25E25T6	Al_{D_1}	330.4	302.7	9.0	0.47	75.5
	Al_{D_2}	331.1	302.6	10.0	0.47	71.4
	Aver.	*330.7*	*302.7*	*9.5*	*0.47*	*73.4*
St-Al.-St DS15E15T6	Al_{E_1}	330.1	300.6	9.1	0.46	69.6
	Al_{E_2}	331.1	300.2	9.5	0.46	70.6
	Aver.	*330.6*	*300.4*	*9.3*	*0.46*	*70.1*
Al-St S25E30P30T6	Al_{F_1}	301.8	273.0	9.5	0.42	68.9
	Al_{F_2}	297.8	264.5	9.1	0.41	70.0
	Aver.	*299.8*	*268.8*	*9.3*	*0.42*	*69.4*
Al-St S30E30P30T6	Al_{G_1}	310.6	273.0	8.6	0.42	63.1
	Al_{G_2}	312.8	275.0	10.2	0.42	71.3
	Aver.	*311.7*	*274.0*	*9.4*	*0.42*	*67.2*
Al-St S30E30G6T3	Al_{H_1}	359.5	318.0	10.3	0.53	66.3
	Al_{H_2}	358.1	315.0	9.3	0.5	76.6
	Al_{H_3}	351.5	309.8	12	0.52	70.1
	Aver.	*356.4*	*314.3*	*10.5*	*0.52*	*71.0*
Design references	CSA-S157	260	240	-	-	70
	AASHT0	290	240	10	-	70
	EC9	290	240	-	-	70

781 Al: aluminum, St: steel
782

783 Table 3. Experimental test results compared to predicted results

Test names	Experimental (aver . load)				EC9 (2007)			AASHTO (2007)			CSA-S157 (2007)		
	1	2	3	4	5	6	7	8	9	10	11	12	13
	P_{exp} (kN)	Std. dev.	P_f (kN)	FM	P_n (kN)	1/5	FM	P_n (kN)	1/8	FM	P_n (kN)	1/11	FM
S15E15T3	22.4	1.09	18.8	S	14.2	1.58	B	14.0	1.60	B	18.7	1.20	S
S15E15T6	39.6	0.66	33.8	S	27.7	1.43	B	28.0	1.41	B	36.6	1.08	S
S15E15T9	57.1	1.04	47.5	S	43.1	1.32	B	44.1	1.29	B	56.7	1.01	S
S15E20T6	52.6	0.56	44.8	N	36.9	1.43	B	37.4	1.41	B	46.3	1.14	N
S25E25T6	69.4	0.68	54.4	B	50.4	1.38	B	40.6	1.71	B	53.3	1.30	B
DS15E15T6	45.6	1.51	35.9	S	30.2	1.51	B	30.1	1.51	B	40.0	1.14	S
S25E30P30T6	95.0	0.83	79.3	N	79.5	1.19	B	72.0	1.32	B	96.7	0.98	N
S30E30P30T6	120.2	0.63	104.1	N	82.7	1.45	B	73.4	1.64	B	100.3	1.20	B
S30E30G60T3	86.84	1.13	63.4	B	65.2	1.33	B	42.08	2.06	B	57.5	1.51	B

784 FM: Failure mode, N: net-section failure; B: bearing failure, S: shear tear-out failure

785

786 Table 4. Experimental versus FE predicted results

	P_{exp} (kN)	Exp. FM	3D P_{FE} (kN)	FE FM	P_{exp}/P_{3DFE}	2D P_{FE} (kN)	P_{exp}/P_{2DFE}
S15E15T3	22.4	S	21.6	S	1.04	20.6	1.09
S15E15T6	39.6	S	39.7	S	0.99	38.0	1.04
S15E15T9	57.1	S	56.4	S	1.01	58.7	0.97
S15E20T6	52.6	N	52.9	N	0.99	47.3	1.11
S25E25T6	69.4	B	71.5	B	0.97	69.8	0.99
DS15E15T6	45.6	S	42.3	S	1.08	41.4	1.10
S25E30P30T6	95.0	N	98.3	N	0.97	102.8	0.92
S30E30P30T6	120.2	N	117.6	N	1.02	115.1	1.04
S30E30G60T3	86.84	B	88.3	B	0.98	85.6	1.01
				Average	1.01		1.03
				Standard deviation	0.04		0.06

787

788

789 Table 5. FE results for one-bolt connection (t=6.35 mm and d=12.7 mm)

One-bolt (1X1) failure load (kN)/failure mode					
			e/d		
s/d	1.5	2	3	4	5
1.5	41.4/S	47.3/N	49.6/N	49.5/N	49.6/N
2	45.7/S	56.2/S	66.3/N	66.5/N	66.8/N
3	43.9/S	58.5/S	79.1/B	89.3/B	90.4/B
4	39.3/S	59.0/S	79.7/B	93.1/B	95.7/B
5	40.4/S	62.2/S	79.8/B	93.0/B	93.8/B

790 N: net-section failure; B: bearing failure, S: shear tear-out failure
791

792 Table 6. FE results for two-bolt connection (t=6.35 mm and d=12.7 mm)

Two-bolt in a column (1X2) FL (kN)/FM						Two-bolt in a row (2X1) FL (kN)/FM					
			p/d						*g/d*		
s/d	*e/d*	2	3	4	5	*s/d*	*e/d*	2	3	4	5
	1.5	48.4/N	48.4/N	48.4/N	48.4/N		1.5	69.0/S	103/S	101/S	96.7/S
	2	48.4/N	48.4/N	48.4/N	48.4/N		2	79.1/N	109N	130/K	133/K
1.5	3	48.4/N	48.4/N	48.4/N	48.4/N	1.5	3	83.9/N	111/N	136/K	152/K
	4	48.4/N	48.4/N	48.4/N	48.4/N		4	84.9/N	112/N	140/N	148/N
	5	48.4/N	48.4/N	48.4/N	48.4/N		5	85.7/N	111/N	140/N	160/N
	1.5	71.5/N	73.0/N	73.0/N	73.0/N		1.5	76.5/S	114/S	109/S	105/S
	2	72.4/N	73.5/N	72.7/N	72.1/N		2	75.9/K	108/K	123/B	122/B
2	3	72.9/N	73.8/N	74.0/N	72.4/N	2	3	91.7/K	125/K	145/B	155/B
	4	73.2/N	73.7/N	72.9/N	72.8/N		4	91.2/K	126/K	148/B	168/B
	5	73.0/N	73.5/N	72.7/N	72.2/N		5	92.0/K	128/K	147/B	168/B
	1.5	88/N	106/N	111/N	111/N		1.5	81.0/S	99.3/S	111/S	120/S
	2	102/N	106/N	112/N	112/N		2	89.7/K	118/K	134/B	153/B
3	3	106/N	115/N	115/N	116/N	3	3	110/K	139/K	159/B	173/B
	4	106/N	116/N	116/N	115/N		4	125/K	156/K	168/B	185/B
	5	109/N	115/N	117/N	115/N		5	135/K	170/K	175/B	184/B
	1.5	93.2/B	111/B	117/B	135/B		1.5	85.6/S	112/S	113/S	115/S
	2	113/B	125/B	138/B	142/B		2	87.2/K	128/K	139/B	133/B
4	3	129/B	137/B	137/B	142/B	4	3	113/K	146/K	160/B	174/B
	4	136/B	137/B	140/B	141/B		4	118/K	154/K	185/B	177/B
	5	137/B	137/B	141/B	143/B		5	123/K	166/K	189/B	172/B
	1.5	90.7/B	105/B	117/B	115/B		1.5	85/S	115/S	114/S	117/S
	2	112/B	133/B	143/B	164/B		2	81.7/K	115/K	130/B	127/B
5	3	132/B	151/B	156/B	162/B	5	3	119/K	146/K	162/B	174/B
	4	154/B	158/B	165/B	180/B		4	128/K	158/K	177/B	176/B
	5	151/B	167/B	165/B	162/B		5	133/K	164/K	180/B	185/B

793 FL: failure load; FM: failure mode; N: net-section failure; B: bearing failure;
794 S: shear tear-out failure; K: block shear faillure
795

796 Table 7. Optimum parameters for one-bolt connection

Bolt grade	*t* (mm)	*d*=12.7 mm		*d*=15.88 mm		*d*=19.05 mm		*d*=25.4 mm	
		e/d	*s/d*	*e/d*	*s/d*	*e/d*	*s/d*	*e/d*	*s/d*
A307	6.35	1.5	1.5	2	1.5	2	1.5	2.5	2.5
	9.53	1.5	1.5	1.5	1.5	1.5	1.5	2	1.5
	12.7	1.5	1.5	1.5	1.5	1.5	1.5	1.5	1.5
	25.4	1.5	1.5	1.5	1.5	1.5	1.5	1.5	1.5
A325	6.35	3	2	3.5	2.5	-	-	-	-
	9.53	2	1.5	2	2	2.5	2.5	4	3
	12.7	1.5	1.5	2	1.5	2	1.5	2.5	2.5
	15.88	1.5	1.5	1.5	1.5	1.5	1.5	2	2
	19.05	1.5	1.5	1.5	1.5	1.5	1.5	2	1.5
	25.4	1.5	1.5	1.5	1.5	1.5	1.5	1.5	1.5
A490	6.35	3	3	-	-	-	-	-	-
	9.53	2	2	3	2	3.5	2.5	-	-
	12.7	1.5	2	2	2	2.5	2	3.5	2.5
	15.88	1.5	1.5	2	1.5	2	1.5	3	2
	19.05	1.5	1.5	1.5	1.5	2	1.5	2	2
	22.22	1.5	1.5	1.5	1.5	1.5	1.5	2	1.5
	25.4	1.5	1.5	1.5	1.5	1.5	1.5	2	1.5

797
798

799 Table 8. Optimum parameters for two-bolt in a column (e=2d)

Bolt grade	t (mm)	d=12.7 mm		d=15.88 mm		d=19.05 mm		d=25.4 mm	
		p/d	*s/d*	*p/d*	*s/d*	*p/d*	*s/d*	*p/d*	*s/d*
A307	6.4	2	2	2	3	2	3	2	4
	9.5	2	1.5	2	1.5	2	2	2	3
	12.7	2	1.5	2	1.5	2	1.5	2	2
	25.4	2	1.5	2	1.5	2	1.5	2	1.5
A325	6.4	3	3	-	-	-	-	-	-
	9.5	2	3	2	3	2	4	-	-
	12.7	2	2	2	3	2	3	2	4
	15.9	2	1.5	2	2	2	3	2	3
	19.1	2	1.5	2	1.5	2	2	2	3
	25.4	2	1.5	2	1.5	2	1.5	2	2
A490	9.5	2	3	3	4	-	-	-	-
	12.7	2	3	2	3	2	4	-	-
	15.9	2	2	2	3	2	3	2	4
	19.1	2	1.5	2	2	2	3	2	3
	22.2	2	1.5	2	2	2	2	2	3
	25.4	2	1.5	2	1.5	2	2	2	3

800
801

802 Table 9. Optimum parameters for two-bolt in row (s=3d)

Bolt grade	t (mm)	d=12.7 mm		d=15.88 mm		d=19.05 mm		d=25.4 mm	
		g/d	*e/d*	*g/d*	*e/d*	*g/d*	*e/d*	*g/d*	*e/d*
A307	6.4	2	1.5	2	1.5	3	1.5	3	3
	9.5	2	1.5	2	1.5	2	1.5	2	2
	12.7	2	1.5	2	1.5	2	1.5	2	1.5
	25.4	2	1.5	2	1.5	2	1.5	2	1.5
A325	6.4	3	2.75	4	3	-	-	-	-
	9.5	3	1.5	3	2	3	3	5	3
	12.7	2	1.5	2	1.5	3	1.5	3	3
	15.9	2	1.5	2	1.5	2	1.5	3	2
	19.1	2	1.5	2	1.5	2	1.5	3	1.5
A490	6.4	4	3	-	-	-	-	-	-
	9.5	4	1.5	4	2	4	3	-	-
	12.7	2	1.5	3	3	3	2	4	3
	15.9	2	1.5	3	1.5	3	1.5	3	3
	19.1	2	1.5	2	1.5	2	1.5	3	2
	22.2	2	1.5	2	1.5	2	1.5	3	1.5

803
804
805